JACS
JOURNAL OF THE AMERICAN CHEMICAL SOCIETY

Article

pubs.acs.org/JACS

Mechanistic Insights into the Bifunctional Non-Heme Iron Oxygenase Carbapenem Synthase by Active Site Saturation Mutagenesis

Ryan M. Phelan and Craig A. Townsend*

Department of Chemistry, Johns Hopkins University, 3400 North Charles Street, Baltimore, Maryland 21218, United Sates

Supporting Information

ABSTRACT: The carbapenem class of β-lactam antibiotics is known for its remarkable potency, antibacterial spectrum, and resistance to β-lactamase-mediated inactivation. While the biosynthesis of structurally "complex" carbapenems, such as thienamycin, share initial biochemical steps with carbapenem-3-carboxylate ("simple" carbapenem), the requisite inversion at C5 and formation of the characteristic α,β-unsaturated carboxylate are different in origin between the two groups. Here, we consider carbapenem synthase, a mechanistically distinct bifunctional non-heme iron α-ketoglutarate-dependent enzyme responsible for the terminal reactions, C5 epimerization and desaturation, in simple carbapenem production. Interestingly, this enzyme accepts two stereoisomeric substrates and transforms each to a common active antibiotic. Owing both to enzyme and product instability, resorting to saturation mutagenesis of active site and selected second-sphere residues gave clearly differing profiles of CarC tolerance to structural modification. Guided by a crystal structure and the mutational data, *in silico* docking was used to suggest the positioning of each disastereomeric substrate in the active site. The two orientations relative to the reactive iron-oxo center are manifest in the two distinct reactions, C5-epimerization and C2/3-desaturation. These observations favor a two-step reaction scheme involving two complete oxidative cycles as opposed to a single catalytic cycle in which an active site tyrosine, Tyr67, after hydrogen donation to achieve bicyclic ring inversion, is further hypothesized to serve as a radical carrier.

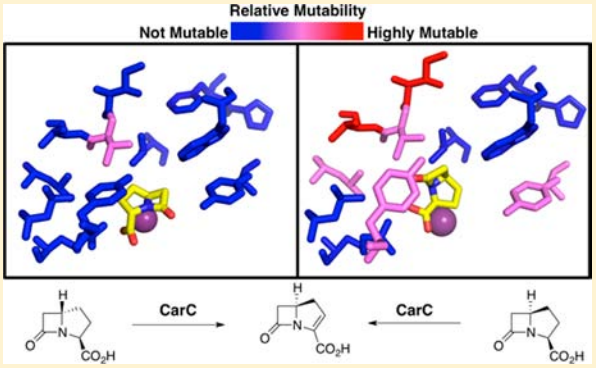

INTRODUCTION

For more than a half century, β-lactam antibiotics, for example, the penicillins and cephalosporins, have held a central place in human medicine combatting infectious diseases and extending lifespans.[1] Over time, however, bacterial resistance to these agents has led to increased reliance on the relatively newer carbapenem class of β-lactams[2] exemplified by key structural elements of thienamycin (**1**) as seen in, e.g., Meropenem **2** and Imipenem **3** (Figure 1a).[3,4] While thienamycin and its naturally occurring homologues are predominantly produced by various species of Actinomycetes, the evolutionarily distant plant pathogen *Pectobacterium carotovorum* produces the simplest member of the family, the bare carbapenem-3-carboxylic acid (**6**) core of this class in a remarkably efficient three-step process (Figure 1b).[5,6] While the first two biosynthetic reactions are shared with thienamycin,[7] the third catalyzed by carbapenam synthase (CarC) is unique to formation of the simple carbapenem **6**. Other presently unknown reactions account for C5 epimerization and C2/3 desaturation in complex carbapenem biosynthesis (see Supplementary Figure 1).

Carbapenem synthase is an unusual member of the α-ketoglutarate (α-KG) dependent dioxygenases. These non-heme iron oxygenases use a canonical His^1-X-Asp/Glu-X_n-His^2 motif together with the bidentate coordination of α-KG, to bind Fe^{II},[8−10] leaving the sixth and sole remaining open site on iron available to coordinate dioxygen. Following ordered substrate and dioxygen binding,[8] oxidative decarboxylation of α-KG produces CO_2, succinate and the highly reactive $iron^{IV}$-oxo (Fe^{IV}=O) intermediate.[11,12] These enzymes are well-known for their ability to react at unactivated C−H bonds typically catalyzing substrate hydroxylation, but epoxidation, desaturation and oxidative cyclization are also known to occur.[9] CarC catalyzes the unprecedented nonoxidative epimerization of (3*S*,5*S*)-carbapenam **4** to (3*S*,5*R*)-carbapenam **5** and desaturation of the latter to the unstable carbapenem **6**.[13] It is known that one of the disastereotopic labels from [5-$^2H_2$,^{13}C]proline (H*) is retained at the bridgehead of **4**, but is lost in the enzyme-catalyzed inversion to **5**.[6] It has been proposed, and recent experimental data support, a radical mechanism in which the active iron-oxo species is generated in conventional manner for this class of enzymes,[11] which abstracts H* of **4** homolytically from the top face of the substrate to give a radical at C5. This bridgehead radical is proposed to be quenched by hydrogen donation from a CarC active site tyrosine residue (Tyr67) located at the back face to form **5** and the tyrosyl radical. The nascent radical is then hypothesized to remove hydrogen from C3 to give the

Received: November 10, 2012
Published: April 23, 2013

dx.doi.org/10.1021/ja311078s | *J. Am. Chem. Soc.* 2013, 135, 7496−7502

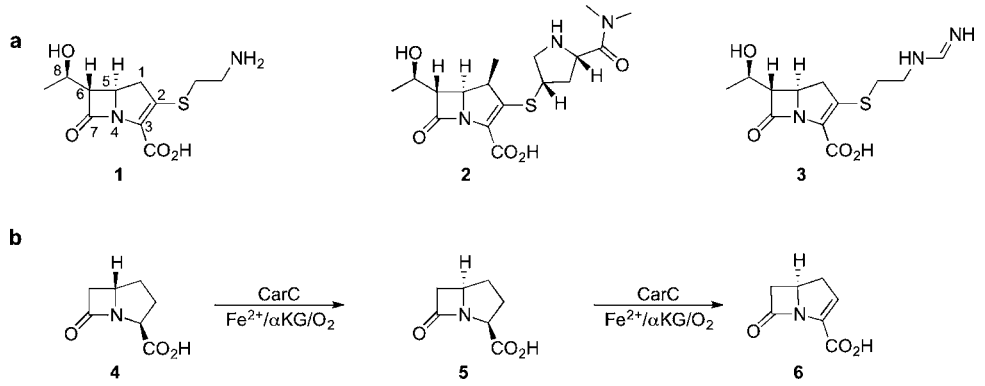

Figure 1. (a) Thienamycin (**1**) and its synthetic, and clinically relevant variants Meropenen (**2**) and Imipenenem (**3**); (b) catalysis of the (3*S*,5*S*)-carbapenam **4** to the intermediate diastereomer **5**, prior to C2−C3 desaturation to yield the active carbapenem **6**.

Scheme 1. Proposed Mechanism for CarC (a) Epimerization and Possible Coupled Desaturation with (3*S*,5*S*)-Carbapenam (4), Full-Reaction and (b) Uncoupled Desaturation with the Previously Epimerized and Released (3*S*,5*R*)-Carbapenam (5), Half-Reaction

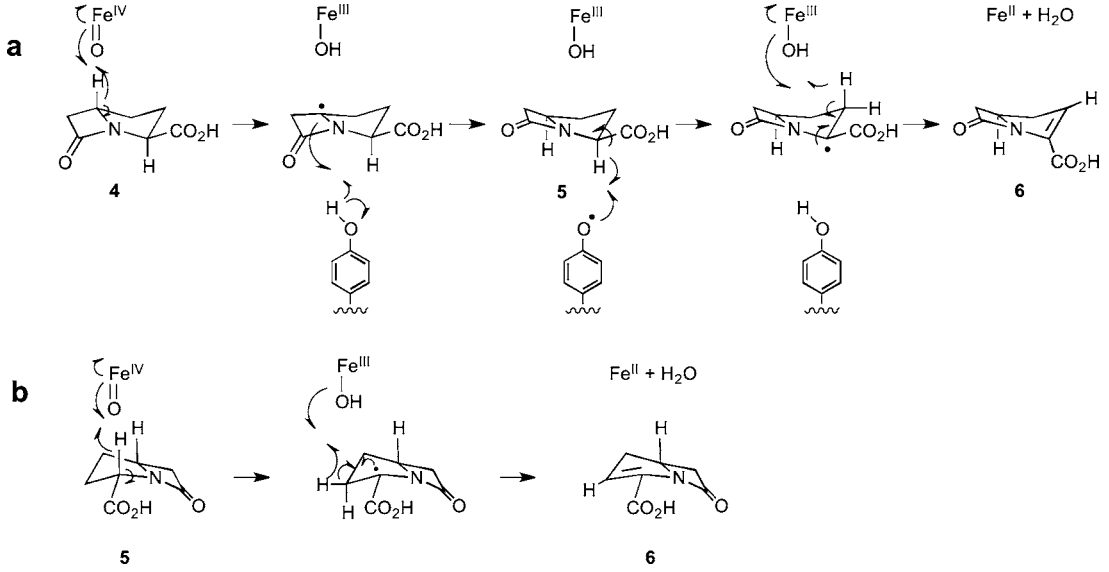

stabilized captodative radical at this site, which then completes the oxidative reaction cycle by [Fe^{III}−OH] mediated scission of a H−C2 bond to accomplish desaturation across C2/3 (Scheme 1). Alternatively, the reaction cycle could be stepwise (i.e., release and reorientation of **5** in the active site for desaturation). In favor of this view is that inverted carbapenam **5** is shown here to be a better substrate for CarC than **4** (*vide infra*) and can be processed independently in a single catalytic cycle.[5] However, such a bifurcated process would require a reduction of the protein or possibly the iron center to occur for stepwise processing to remain catalytic. It is not known how such an overall reaction would occur although reduction of tyrosyl radicals by, for example, glutathione is precedented.[14]

As appealing as the tyrosyl-mediated radical mechanism is to achieve bridgehead inversion in a stoichiometric and thermodynamically plausible manner,[15] quite considerable stereochemical and conformational changes must occur in CarC to accommodate the interconversion of **4** to **6**, as depicted in Scheme 1. Investigation of the CarC mechanism is unfortunately thwarted by both protein instability and product lability,[13] which greatly limits the stoichiometric, kinetic and labeling methods that can be applied. Mechanistic studies, which are largely unavailable for CarC, would not only provide insight into enzyme function but also could prove valuable to the modification and improvement of enzyme activity.[16] To obtain insight into this unique process, a conceptually different approach was needed. A demonstrated alternative to conventional kinetic analysis is combinatorial or saturation mutagenesis, which allows all amino acid substitutions at selected loci to be evaluated, thus providing a more comprehensive picture of the overall contribution of each residue. This strategy has been used to study enzyme mechanism,[17−21] quaternary structure[22,23] and substrate specificity.[24]

To gain greater mechanistic understanding of CarC, we applied our recently described fluorescence screening assay[25] (Scheme 2) with the aim to better define the reactivity of the CarC Fe^{IV}=O intermediate, which is governed by the geometry of the active site and second-sphere residues, and further dictated by the protein's conformational landscape.[26] Residues composing the active site orient the substrate to ensure proper wave function overlap between the reactive Fe^{IV}=O/Fe^{III}−OH intermediate and the substrate. Recent studies have demonstrated how even small reductions of steric bulk in the active site of the nonheme α-KG-dependent iron

dx.doi.org/10.1021/ja311078s | J. Am. Chem. Soc. 2013, 135, 7496−7502

Scheme 2. Fluorescence Assay for the Detection of β-Lactam Antibiotics Mediated by pRP5.199[a]

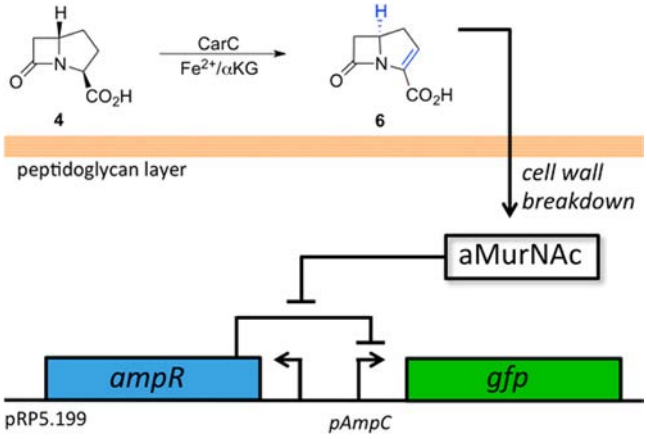

[a]As **4** (or intermediate **5**) is catalyzed into the antibiotic-active **6**, peptidoglycan breakdown occurs, eventually resulting in production of the *N*-acetyl anhydro-Muramic Acid pentapeptide (aMurNAc). aMurNAc binds to AmpR allowing transcription of the gene(s) downstream from the *ampC* promoter (*pAmpC*), in this case *gfp*.

dioxygenase taurine α-ketoglutarate dioxygenase (TauD) increases substrate conformational sampling, thus lessening productive hydrogenic wave function overlap with the Fe^{IV}=O center and greatly diminishing catalytic activity.[27,28] Similar results have been observed with a mechanistically distinct, but related iron dioxygenase, soybean lipoxygenase-1 (SLO-1).[29−31] Bearing these observations in mind, the ability to examine separately both the complete two-step reaction (**4** → **6**) and the second half-reaction (**5** → **6**) provided a unique opportunity to evaluate and compare the functional robustness of the CarC active site to other, simpler, α-KG-dependent dioxygenase reactions. Two sets of distinct results were obtained that were applied to generate a computational model to further account for the observed amino acid tolerance and suggest binding orientations for **4** and **5** that analysis of the crystal structure alone could not unambiguously assign. In aggregate, our experiments aimed to determine the molecular underpinnings that enable CarC to regio- and stereospecifically carry out two distinct reactions (coupled or uncoupled epimerization and desaturation). These findings simultaneously provided mechanistic and structural insights into this important class of enzymes, and further defined active site plasticity for each reaction.

RESULTS

Generation and *in Vivo* Screening of CarC Mutants. To select the active site and second-sphere residues for mutational analysis, we first examined the crystal structure of CarC to identify those that were in direct contact with the substrate analog, *N*-acetyl proline (Table 1).[10] Following their identification, we selected second-sphere residues that appeared to be in close contact with more than one inner sphere residue, hence, further defining the active site through their steric bulk and buttressing effects. Together, six active site and four second sphere residues were identified for mutational analysis. As previously reported, Tyr67 was targeted to investigate its possible role as the hydrogen donor involved in epimerization of the (3*S*,5*S*)-carbapenam **4** to its C5 epimer **5**.[25] This choice stemmed from inspection of the crystal structure, which showed that a minor shift of less than 2.5 Å by Tyr67 would make it a candidate for the proposed radical shuttle required in the coupled reaction of 4 to 6. Proline 193 was selected to determine if it played a role in positioning the carbonyl of Phe192 to aid in stabilizing and orienting Trp202 for pi-stacking interactions with aromatic residues Tyr191 and Phe194.

CarC variants were screened using an assay in which production of a β-lactam antibiotic elicits a fluorescent response from an engineered *Escherichia coli* (Scheme 2).[25] The assay has been shown to be acutely sensitive to the presence of β-lactam antibiotics and highly reproducible. Additionally, this assay demonstrated a graded response to β-lactam concentration, which allowed for ranking and comparison of CarC variant activity. Each point- or double mutant library was screened with >95% certainty that all codons were represented. Colonies exhibiting fluorescence 2-fold greater than the background signal (approximately 5% of wild-type activity) were picked and sequenced. All CarC single mutant strains were screened for catalytic activity with both the native substrate, (3*S*,5*S*)-carbapenam **4** and the intermediate diastereomer, (3*S*,5*R*)-carbapenam **5** (Table 1), while CarC double mutants, Y191X/W202X' and F194X/W202X', were screened with **4**. The instability[32] of **6** precluded the direct correlation of fluorescence to carbapenem concentration; therefore, to correct for the nonlinear fluorescence response[25] all signals were

Table 1. Residues Found To Complement the CarC Reaction of 4 to 6 and 5 to 6 with the Percentage of Wild-Type Activity Listed and the Associated Standard Deviation of Fluorescence

CarC A.A.	4 → 6	5 → 6
Y67[a]	Y	Y; F(14.5)[b], W(13.3 ± 1.3)
L82	L	L
L84[c]	L	L; M(16.1 ± 4.1); V(9.0 ± 3.1)
T93[c]	T	T; C(84.7 ± 12.5); G(63.4 ± 7.8); S(56.5 ± 8.4); Ala(53.3 ± 9.9); N(17.2 ± 1.1): V(13.3 ± 0.2); D (13.3 ± 3.1)
I91[c]	I	I; S(82.3 ± 11.2); V (80.0 ± 9.2); A(56.5 ± 3.8); C(46.9 ± 7.9); L(15.8; 3.8); T(14.5 ± 1.2)
V92	V, I(61.8 ± 18.0)	V; I(89.9 ± 4.4)
L98	L	L
Y191	Y	Y; F(46.8 ± 7.6)
P193	P	P
F194[c]	F	F
W202	W	W
R267	R	R

[a]Proposed catalytic tyrosine. [b]Only one colony found, no standard deviation available. [c]Residue located in the second sphere of the active site.

converted to represent fractions of wild-type activity as amoxicillin equivalents using a standard calibration curve.

Analysis of the CarC Binding Pocket with (3*S*,5*S*)-Carbapenam 4 (Full Reaction). With regard first to the reaction of substrate **4**, initial inspection of the data reveals the intractability of CarC toward mutation in the immediate vicinity of the active site. Only one residue demonstrated mutability, Val92. The sole acceptable alteration found, V92I, is a conservative mutation, which underscores the importance of an aliphatic, β-branched, amino acid at this site. We believe that this β-branching plays a central role in proper packing of the substrate in the active site for C5 hydrogen abstraction. The third β-branched amino acid, Thr, did not emerge in the screen as a viable replacement for Val92, but it might be assumed that inserting a hydroxyl in the active site could interfere with the catalytic cycle by introduction of a polar, hydrogen bond donor. Inspection of the remaining first and second sphere residues demonstrates how their particular steric attributes are necessary for positioning of the substrate.

Unsurprisingly, Arg276 was found to be immutable. This result was expected as inspection of the CarC crystal structure revealed the high probability that this residue forms an ion pair with the bound substrate mimic carboxylate, and therefore, likely interacts with the substrate carboxylate during catalysis. Added support for this proposal can be found in the CarC homologue clavaminate synthase where Arg297 interacts with its substrate in this fashion.[33]

Analysis of the CarC Binding Pocket with (3*S*,5*R*)-Carbapenam 5 (Second Half-Reaction). In keeping with the mutational analysis of **4**, Arg267, and the neighboring aromatic residues Tyr191-Trp202-Phe194, are conserved. Notably, however, Tyr191 can be replaced with Phe in the second-half reaction, indicating the necessity for the aryl hydroxyl in the complete, but not second-half reaction. This difference notwithstanding, the Y191F substitution still retains the edge-to-face phenyl-indole-phenyl motif. Additional inspection of the mutational results reveals a general increase in tolerance for residue variation in the adjacent active-site and second-sphere residues, although the extent of mutability appears to still be limited to a small subset of highly similar amino acids. In a departure from the rigid requirements of the full-reaction, the second sphere residues Ile91 and Thr93 display a marked increase in mutability in the second-half reaction. Isoleucine 91 tolerated substitution with all small aliphatic residues, except glycine and proline, including those containing a hydroxyl group. Threonine 93 also exhibited surprising mutability, with the capacity to substitute all hydroxyl-containing residues as well as glycine with retention of wild-type catalytic activity. To a lesser extent, the small hydrophobic residues, Ala and Val, and even to two similar more polar residues, Gln and Glu, complemented the reaction. As observed with **4**, substrate **5** does require that specific residues remain invariant to properly position C2 and C3 over the iron center. Unlike the catalysis of **4**, residues distal to **5** are inherently more mutable, likely a reflection of the comparative ease of desaturation versus coupled epimerization and desaturation.

Pairwise Mutational Analysis of Aromatic Interactions (Tyr191-Trp202-Phe194). Surprised by the functional immutability observed in the triad of aryl residues for the full reaction, we sought to further probe their interactions by sampling a larger mutational space to determine if potentially synergistic, pairwise combinations could replace residues in this region. Two double mutant libraries were created, Y191X/W202X' and F194X/W202X', which were screened for catalysis with **4**. It was observed that no pairwise mutations could replace the aromatic interactions found in this region. These interactions appeared to be important for the reaction, a likely structural element of the enzyme forming an "aromatic wall" along one side of the active site.

As Tyr191 and Phe194 are located in the interior of the protein, parallel to one another, the polypeptide chain extends to a β-turn at which point it protrudes from the interior of the enzyme and projects over the surface of the protein (Figure 2).

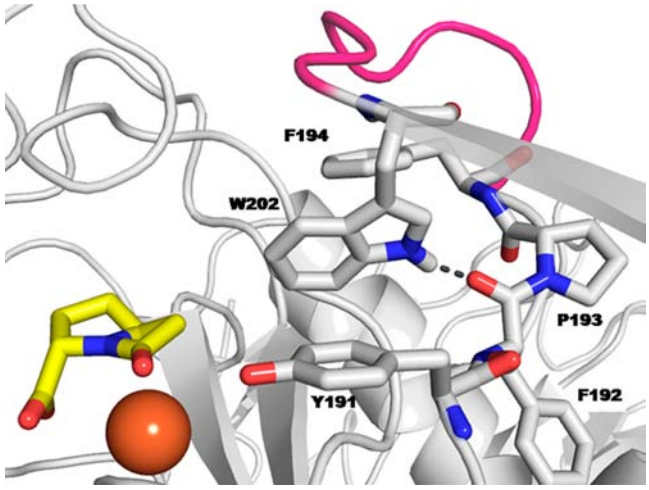

Figure 2. Aromatic region consisting of the edge-to-face-to-edge π-stacking interactions of Y191, W202 and F194. P193 positions the carbonyl of F192 for hydrogen bonding of the indole N−H on W202. The β-turn is highlighted in magenta and iron center in orange.

Following the β-turn the polypeptide chain wraps back through the Tyr191/Phe194 region with Trp202 inserting itself between these residues in a perpendicular fashion. The crystal structure additionally shows the indole N−H of Trp202 is hydrogen-bonded to the carbonyl of Phe192. Such an interaction, being located in a nonpolar environment, has been demonstrated to be stronger than a solvent exposed hydrogen bond.[34] The mutational data assert that Pro193 is essential for both reactions, likely positioning the carbonyl of Phe192 for hydrogen bonding with Trp202 as it is invariant in both the full- and half-reaction. This reasoning is supported by the crystal structure. In sum, the hydrogen bonding interactions of Trp202 with the F192 carbonyl and edge-to-face pi interactions between the aromatic residues are expected to provide a significant thermodynamic contribution to both the local and overall stability of this protein. Removal of these interactions clearly results in perturbation of the active site that adversely affects substrate−protein interactions critical for preserving catalytic activity.

Computational Modeling of Bound Substrates. Taking into account proposed mechanisms for CarC,[2S,3S] the known stereochemical requirements for the reaction[5,6] and the new mutational data, we applied computational modeling in the context of the previously reported crystal structure[36] to create a clearer picture of substrate binding and catalysis. To catalyze the full reaction, it is proposed that hydrogen abstraction from C5 would occur by way of the Fe^{IV}=O center creating a C5 radical, which could be quenched on the opposite face by Tyr67, which is located on a mobile loop over the active site

dx.doi.org/10.1021/ja311078s | J. Am. Chem. Soc. 2013, 135, 7496−7502

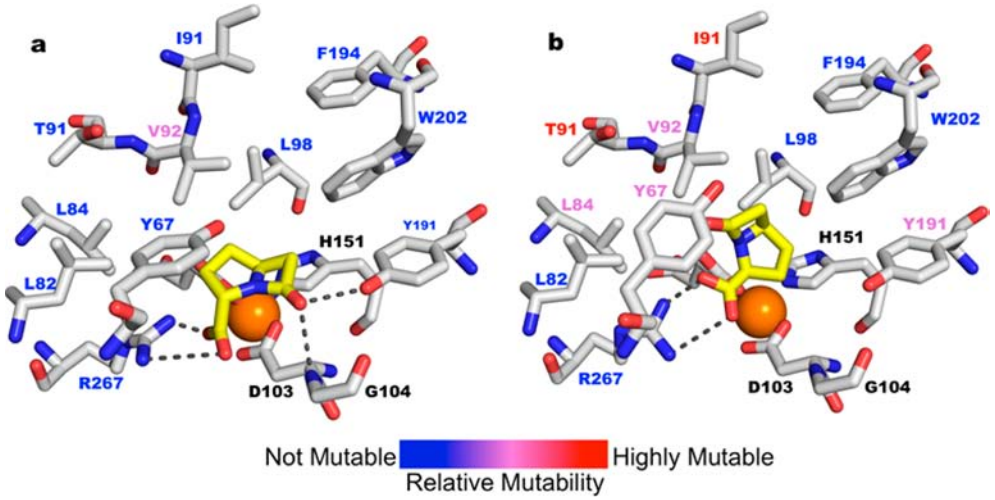

Figure 3. (a) Model of (3*S*,5*S*)-carbapenam in the CarC active site; (b) model of (3*S*,5*R*)-carbapenam in the CarC active site. Color coded labels indicate the relative mutability of selected active site residues, residue labels in black were not investigated. Iron center colored in orange.

(epimerization of **4** to **5**). The newly formed tyrosyl radical is then proposed to abstract hydrogen from C3 forming a delocalized α-radical. The Fe^{III}−OH intermediate can next abstract hydrogen from C2 to create the α,β-unsaturated carboxylate, (Scheme 1a). Conversely, direct desaturation of C2−C3 (second half-reaction) would require that C3 be accessible to the Fe^{IV}=O (or Fe^{III}−OH) intermediate. If **5** were to reside in the active site in an orientation similar to that of **4**, the C3 hydrogen would be blocked by the C3 carboxylate. With the substrate C3 carboxylate likely binding Arg267, the carbapenam must rotate ∼180° to simultaneously present the C2 and C3 hydrogens for abstraction by the iron-oxo intermediate(s) (Scheme 1b). Taking these mechanistic and geometric considerations into account, we suggest that these two substrates fit in the active site in distinctly different orientations. Models generated of the active site containing each of these two substrates were refined in accordance with our mutational data (Figure 3; Supplementary Figure 2 shows active sites in stereo view and Supplementary Figure 3 in more detailed color).

Substrates **4** and **5** were docked in the active site guided by the chemical and mutational data. Constraints were set to properly position the substrate over the iron center and place Tyr67 at an acceptable distance for reaction with the substrate. The ensemble was minimized using CHARMm[37] to reduce unfavorable steric interactions and energy-minimize the structures. Each model was manually refined to allow interaction of the substrate and residues that have been shown to be critical for catalysis.

DISCUSSION

The combined data from the epimerization reaction parallel previous studies that demonstrated how diminishing steric bulk in the active site of TauD and SLO-1 greatly reduced catalytic efficiency.[27−31] While the transition state of the TauD hydroxylation reaction requires the overlap of the Fe^{IV}=O and C−H wave functions for hydrogen abstraction, CarC has a more restrictive set of transition states where the same Fe^{IV}=O and C−H interaction is not only needed, but also requires delivery of hydrogen from the opposite face, likely by Tyr67. Proper overlap of these three component wave functions would presumably be even more acutely dependent on precise substrate positioning, derived from the active site architecture, and is, therefore, as, if not more, affected by geometric changes than a simple hydroxylation or dioxygenase reaction. These constraints are clearly reflected in the mutation profile with **4**.

It is anticipated that for uncoupled desaturation (**5** → **6**) to occur the C2 and C3 hydrogens should both be accessible to the Fe^{IV}=O/Fe^{III}−OH center. To account for this difference in mechanism, substrate **5** must be rotated ∼180° around the C3-carboxylate-Arg267 ion pair axis. Our model suggests that, as rotation occurs, the β-lactam moiety moves away from the aromatic triad (Tyr191-Trp202-Phe194) toward Val92 and Leu98. These residues reside in a region of the enzyme where the majority of active site and second sphere residues are small and hydrophobic. While many of these residues are mutable, Leu98 is not and Val92 only tolerates the conservative V92I mutation. Thus, it appears that their steric bulk is essential for proper orientation of **5** over the iron center. When combined, the results for the second half-reaction show that alteration of the CarC active site and second-sphere residues is better tolerated, particularly in the second sphere. This limited structural flexibility notwithstanding, some regions remain invariant paralleling the profile for the complete reaction, such as Arg267, Leu98, Val92/V92I and the aromatic triad, hence, defining a subset of residues important for overall catalytic integrity. These data are in accord with our understanding of this class of enzymes as it catalyzes stereo- and regiospecific C−H activation; proper alignment over the iron center, therefore, is critical.

One perplexing observation was the necessity for both Tyr67 and Tyr191 in the complete reaction, while the hydroxyl moiety of these residues appeared to be only marginally beneficial in the second-half reaction. To account for these sharp differences we employed our model generated from the crystal structure and mutational data in an attempt to formulate a plausible mechanistic explanation. In the CarC crystal structure the substrate mimic, *N*-acetyl proline, sits in the active site with no hydrogen bond acceptor extending toward Tyr191, while Tyr191 is involved in a hydrogen bonding interaction with the Gly104 carbonyl. In our model, **4** is proposed to reside in the active site with the β-lactam carbonyl extending in the direction of Tyr191. We propose that as the substrate enters the active site, a subtle rearrangement occurs with the hydrogen-bonding

dx.doi.org/10.1021/ja311078s | *J. Am. Chem. Soc.* 2013, 135, 7496−7502

interaction of Tyr191 and Gly104 broken in favor of forming two hydrogen bond donors to the β-lactam carbonyl (Supplementary Figure 2a). This dual hydrogen bond, consisting of the Tyr191 O−H and Gly104 N−H, would help to further orient the substrate and stabilize it in the active site. Knowing that the full-reaction is highly sensitive to correct substrate geometry, these additional hydrogen-bonding interactions would be valuable to lock the proper orientation of **4**. Inspection of the half-reaction **5** → **6** shows that the Tyr191 O−H is not needed; only an aromatic phenyl ring is required. This result makes chemical sense as both Tyr and Phe have been demonstrated to make equal contributions when engaged in edge-to-face pi interactions[38] and fits with our model, as the β-lactam carbonyl in the model of **5** does not extend toward Tyr191. This hydrogen bonding interaction, therefore, would not be required as it was in the full-reaction (Supplementary Figure 2b). This leaves Tyr67 available to fulfill its proposed role as the catalytic tyrosine participating in epimerization and potentially as a radical shuttle. Further support for the role of Tyr67 as the catalytic tyrosine lies in the fact that Tyr191 appears to be oriented in the plane of the carbapenem, as opposed to in line with the Fe^{IV}=O center and C5; its position in the active site would therefore preclude involvement in catalysis in accord with the model.

With regard to the transformation of **4** to **6**, two chemically and thermodynamically plausible mechanisms exist to account for catalysis. It has been proposed that CarC could carry out this reaction using coupled epimerization and desaturation, which involves the intriguing proposal that Tyr67 behaves as a radical carrier to sustain a single catalytic cycle. This, however, would require exquisite precision in coupled protein motions to optimally and rapidly align multiple wave functions for the proposed radical shuttle to efficiently operate on C5 and C3. On the other hand, it is entirely likely that this enzyme predominantly uses a stepwise process in which the putative tyrosyl radical is reductively quenched and the enzyme reloads α-KG, the bridgehead-inverted intermediate **5** and dioxygen to carry out desaturation to carbapenem **6** in a second step. While at present it is not possible to exclude the first mechanism as at least partially participating, several lines of evidence favor the stepwise process. First, in *in vitro* and *in vivo* experiments, the inverted carbapenam **5** is always observed and predominates over carbapenem **6**. The relatively lower amounts of **6** could be at least partially mitigated by the fact that it is hydrolytically unstable and degrades as it is formed in any experiment. Further to this point, however, is that **5** is, in fact, a superior substrate to **4** for CarC. In contrast to previous reports,[39] use of our assay conditions reported earlier[25] revealed that **5** produces approximately 300% (see Supporting Information) more product (**6**) than does substrate **4** in keeping with better k_{cat}/K_m characteristics. Third, and perhaps most compelling, are the mutational results presented here that establish that the tolerance for CarC active site structural alteration is markedly different for **4** and **5**, even in the face of the inescapable geometric constraints of iron−oxygen mediated catalysis. The severity of physical change in the substrate upon bridgehead inversion and its requirement for plausible alignment with the transiently formed Fe(IV)=O/Fe(III)−OH species are more readily appreciated in 3D (see Supplementary Figure 2). In our view, the apparent 180° rotation required in the active site giving rise to frequent aborted cycles might best be accommodated by release and rebinding of **5** to complete desaturation in a second cycle. Such multistep behavior by members of the α-KG dependent oxygenases is precedented, notably by clavaminate synthase.[40]

■ CONCLUSION

CarC is a unique member of the α-KG dependent, non-heme iron oxygenases that catalyzes substrate epimerization and desaturation in either separate or coupled reactions. We approached the study of this enzyme with the goal to understand in greater detail the overall mechanism of this pivotal transformation in carbapenem biosynthesis, and subsequently apply that understanding to the engineering of this protein for the preparation of structurally modified carbapenem antibiotics. In the face of both enzyme instability and high product lability, we opted to perform saturation mutagenesis on selected residues in and adjacent to the active site to deduce both residue tolerance and their role in substrate binding and catalysis. In keeping with the complexity of the overall reaction, the mutational analysis shows that constraints on the shape and polarity of the active site are high, and the distance requirements to the iron-oxo center and Tyr67 are key to any contemplated engineering efforts. Furthermore, we were able to illuminate differences in the mutational profiles between the full and second half-reactions that underscore the relative difficulty of each reaction and favor stepwise epimerization and desaturation events in the biosynthesis of the core carbapenem **6**.

■ EXPERIMENTAL METHODS

pRP5.199 Fluorescence Assay. CarC variants contained in pDIMC8K were transformed into *E. coli* SN0301 (hereafter referred to as *E. coli* RP3). *E. coli* RP3was grown for 24 h on 2xYT containing 1.0% (w/v) glycerol and the resultant colonies were transferred to LB + 1.0% glycerol with tetracycline (5 μg/mL), kanamycin (25 μg/mL), ferric ammonium sulfate (80 μM) and 500 μM (3*S*,5*S*)-carbapenam or 250 μM (3*S*,5*S*)-carbapenam using sterile applicators. The assay plate was grown at 37 °C for 16 h. After growth of the colonies, the plate fluorescence was read on a General Electric Typhoon 9140 phosphorimager using λ_{ex} = 488 nm, λ_{em} = 525 nm with +3.0 mm top focusing. The data were analyzed using ImageQuant TL (GE Lifesciences). All colonies exhibiting fluorescence greater than 5% of wild-type were recorded and sequenced as active clones.

Quantitative Analysis of pRP5.199 Trial Assay. After fluorescence was read, the data were analyzed using ImageQuant TL (GE Lifesciences, Piscataway, NJ). Each colony was interrogated separately using correction for background fluorescence. Arbitrary fluorescence units were recorded for each colony. The average of *E. coli* SN0301 with pDIMC8K-MalE was used to determine fluorescence intensity attributed to the basal transcription of *gfp* on pRP5.199. Wild-type activity was determined by using pDIMC8K-CarAC as the positive control.

Computational Modeling of (3*S*,5*S*)-Carbapenam and (3*S*,5*R*)-Carbapenam in the CarC Active Site. All computational work was performed using Accelrys Discovery Studio 2.1 suite (San Diego, CA). The carbapenem was created using the Discovery Studio drawing function and energy minimized using the Smart Minimizer program. The substrate was manually docked in the CarC (pdb ID: 1NX8) B-subunit active site. Constraints were set for the (3*S*,5*S*)-carbapenam so that the iron-oxo center would be within 2.75−3.25 Å of the carbapenam C5 and a further constraint was to set the tyrosyl hydroxyl at 2.75−3.25 Å. For the (3*S*,5*R*)-carbapenam, the iron-oxo center was set to be within 2.75−3.25 Å of both the carbpenam C2 and C3. The system was typed with the 3 CHARMm[37] algorithm and minimized using an adopted basis NR algorithm with a generalized Born implicit solvent model with molecular volume. The resultant minimized model was visualized using PyMol.

dx.doi.org/10.1021/ja311078s | *J. Am. Chem. Soc.* 2013, 135, 7496−7502

Correction for Nonlinear Fluorescence Response. A calibration curve of amoxicillin from 15.2 to 500.0 ng/mL was generated as previously reported.[25] Identical plates were prepared using standard assay conditions containing **4** or **5** (1.0 mM) and plated with *E. coli* RP3 cells. Fluorescence was read for the amoxicillin standards as well as plates containing **4** or **5**. The amoxicillin response was fit to a logarithmic function. Solving of that function for fluorescence allowed conversion of CarC activity (with both **4** and **5**) to known amoxicillin concentrations. It was determined wild-type CarC activity with **4** and **5** corresponded to 70.4 and 202.4 ng/mL, respectively. Fractions of wild-type activity obtained from CarC mutants were compared using the linear amoxicillin equivalent scale.

■ ASSOCIATED CONTENT

Ⓢ Supporting Information

Experimental detail; correction for nonlinear fluorescence with **4** and **5**; tables of oligonucleotides and corrected fluorescence and the calculated amoxicillin equivalents of **4** and **5** when catalyzed by wtCarC; scheme of (3*S*,5*S*)-carbapenam formation in the biosynthesis of both the simple carbapenem and thienamycin; stereoview images of the (3*S*,5*S*)-carbapenam and (3*S*,5*S*)-carbapenam; tolerance of CarC active site to mutation with (3*S*,5*S*)-carbapenam and (3*S*,5*R*)-carbapenam; amoxicillin calibration curve. This material is available free of charge via the Internet at http://pubs.acs.org.

■ AUTHOR INFORMATION

Corresponding Author

ctownsend@jhu.edu

Notes

The authors declare no competing financial interest.

■ ACKNOWLEDGMENTS

We are grateful to Dr. R. Li for discussions concerning this work, A. R. Buller for assistance with computer graphics, Dr. J. W. Labonte for help with computational modeling. This work was supported by a grant from The National Institutes of Health (AI014937).

■ REFERENCES

(1) Andersson, I.; van Scheltinga, A. C.; Valegard, K. *Cell. Mol. Life Sci.* **2001**, *58*, 1897.
(2) Ramphal, R. *Crit. Care* **2008**, *12* (4), S1.
(3) Nicolau, D. P. *Expert Opin. Pharmacother.* **2008**, *9*, 23.
(4) Bodner, M. J.; Phelan, R. M.; Freeman, M. F.; Li, R.; Townsend, C. A. *J. Am. Chem. Soc.* **2010**, *132*, 12.
(5) Stapon, A.; Li, R.; Townsend, C. A. *J. Am. Chem. Soc.* **2003**, *125*, 15746.
(6) Stapon, A.; Li, R.; Townsend, C. A. *J. Am. Chem. Soc.* **2003**, *125*, 8486.
(7) Bodner, M. J.; Li, R.; Phelan, R. M.; Freeman, M. F.; Moshos, K. A.; Lloyd, E. P.; Townsend, C. A. *ChemBioChem* **2011**, *12*, 2159.
(8) Zhou, J.; Kelly, W. L.; Bachmann, B. O.; Gunsior, M.; Townsend, C. A.; Solomon, E. I. *J. Am. Chem. Soc.* **2001**, *123*, 7388.
(9) Hausinger, R. P. *Crit. Rev. Biochem. Mol. Biol.* **2004**, *39*, 21.
(10) Zhou, J.; Gunsior, M.; Bachmann, B. O.; Townsend, C. A.; Solomon, E. I. *J. Am. Chem. Soc.* **1998**, *120*, 13539.
(11) Grzyska, P. K.; Appelman, E. H.; Hausinger, R. P.; Proshlyakov, D. A. *Proc. Natl. Acad. Sci. U.S.A.* **2010**, *107*, 3982.
(12) Price, J. C.; Barr, E. W.; Tirupati, B.; Bollinger, J. M., Jr.; Krebs, C. *Biochemistry* **2003**, *42*, 7497.
(13) Parker, W. L.; Rathnum, M. L.; Wells, J. S., Jr.; Trejo, W. H.; Principe, P. A.; Sykes, R. B. *J. Antibiot.* **1982**, *35*, 653.
(14) Sturgeon, B. E.; Sipe, H. J., Jr.; Barr, D. P.; Corbett, J. T.; Martinez, J. G.; Mason, R. P. *J. Biol. Chem.* **1998**, *273*, 30116.
(15) Topf, M.; Sandala, G. M.; Smith, D. M.; Schofield, C. J.; Easton, C. J.; Radom, L. *J. Am. Chem. Soc.* **2004**, *126*, 9932.
(16) Toscano, M. D.; Woycechowsky, K. J.; Hilvert, D. *Angew. Chem., Int. Ed. Engl.* **2007**, *46*, 3212.
(17) Kast, P.; AsifUllah, M.; Jiang, N.; Hilvert, D. *Proc. Natl. Acad. Sci. U.S.A.* **1996**, *93*, 5043.
(18) Kast, P.; Hartgerink, J. D.; AsifUllah, M.; Hilvert, D. *J. Am. Chem. Soc.* **1996**, *118*, 3069.
(19) Kunzler, D. E.; Sasso, S.; Gamper, M.; Hilvert, D.; Kast, P. *J. Biol. Chem.* **2005**, *280*, 32827.
(20) Yep, A.; Kenyon, G. L.; McLeish, M. J. *Proc. Natl. Acad. Sci. U.S.A.* **2008**, *105*, 5733.
(21) Wilming, M.; Iffland, A.; Tafelmeyer, P.; Arrivoli, C.; Saudan, C.; Johnsson, K. *ChemBioChem* **2002**, *3*, 1097.
(22) MacBeath, G.; Kast, P.; Hilvert, D. *Science* **1998**, *279*, 1958.
(23) MacBeath, G.; Kast, P.; Hilvert, D. *Protein Sci.* **1998**, *7*, 1757.
(24) Ang, E. L.; Obbard, J. P.; Zhao, H. *FEBS J.* **2007**, *274*, 928.
(25) Phelan, R. M.; Dipardo, B. J.; Townsend, C. A. *ACS Chem. Biol.* **2012**, *7*, 835.
(26) Nagel, Z. D.; Klinman, J. P. *Nat. Chem. Biol.* **2009**, *5*, 543.
(27) McCusker, K. P.; Klinman, J. P. *J. Am. Chem. Soc.* **2010**, *132*, 5114.
(28) McCusker, K. P.; Klinman, J. P. *Proc. Natl. Acad. Sci. U.S.A.* **2009**, *106*, 19791.
(29) Meyer, M. P.; Tomchick, D. R.; Klinman, J. P. *Proc. Natl. Acad. Sci. U.S.A.* **2008**, *105*, 1146.
(30) Knapp, M. J.; Rickert, K.; Klinman, J. P. *J. Am. Chem. Soc.* **2002**, *124*, 3865.
(31) Knapp, M. J.; Klinman, J. P. *FEBS* **2002**, *269*, 3113.
(32) Parker, W. L.; Koster, W. H.; Cimarusti, C. M.; Floyd, D. M.; Liu, W. C.; Rathnum, M. L. *J. Antibiot.* **1982**, *35*, 189.
(33) Zhang, Z.; Ren, J.; Stammers, D. K.; Baldwin, J. E.; Harlos, K.; Schofield, C. J. *Nat. Struct. Biol.* **2000**, *7*, 127.
(34) Gao, J.; Bosco, D. A.; Powers, E. T.; Kelly, J. W. *Nat. Struct. Mol. Biol.* **2009**, *16*, 684.
(35) Borowski, T.; Broclawik, E.; Schofield, C. J.; Siegbahn, P. E. *J. Comput. Chem.* **2006**, *27*, 740.
(36) Clifton, I. J.; Doan, L. X.; Sleeman, M. C.; Topf, M.; Suzuki, H.; Wilmouth, R. C.; Schofield, C. J. *J. Biol. Chem.* **2003**, *278*, 20843.
(37) Brooks, B. R.; Bruccoleri, R. E.; Olafson, B. D.; States, D. J.; Swaminathan, S.; Karplus, M. *J. Comput. Chem.* **1983**, *4*, 187.
(38) Serrano, L.; Bycroft, M.; Fersht, A. R. *J. Mol. Biol.* **1991**, *218*, 465.
(39) Sleeman, M. C.; Smith, P.; Kellam, B.; Chhabra, S. R.; Bycroft, B. W.; Schofield, C. J. *ChemBioChem* **2004**, *5*, 879.
(40) Janc, J. W.; Egan, L. A.; Townsend, C. A. *J. Biol. Chem.* **1995**, *270*, 5399.